



ISSN 1349-1113
JAXA-RR-04-023E

JAXA Research and Development Report

Non-contact property measurements of liquid and supercooled ceramics with a hybrid electrostatic-aerodynamic levitation furnace

Paul-François PARADIS, Takehiko ISHIKAWA
and Shinichi YODA

March 2005

Japan Aerospace Exploration Agency

Non-contact property measurements of liquid and supercooled ceramics with a hybrid electrostatic-aerodynamic levitation furnace

By

Paul-François Paradis,¹ Takehiko ISHIKAWA, Shinichi YODA

Abstract:The use of an hybrid pressurized electrostatic-aerodynamic levitation furnace and procedures developed by the Japan Aerospace Exploration Agency overcame the contamination problems associated with the processing of ceramics under extreme temperature conditions. This made possible property measurements over wide temperature ranges that cover the superheated as well as the supercooled states. In this study, samples of various ceramics were levitated and their densities were found as a function of temperature by extracting the area from images of a UV backlit axi-symmetric sample of known mass. In addition, the work function of each molten material was estimated using the Richardson-Dushman equation.

Keywords : ceramics, containerless processing, density, electrostatic levitation, liquid, supercooling, work function.

1. Introduction

Ceramics such as $\text{Nd-CaAl}_2\text{O}_4$ (Nd-CA), $\text{Y}_3\text{A}_{15}\text{O}_{12}$ (YAG), BiFeO_3 , and BaTiO_3 are interesting for numerous optical (e.g. IR windows, fibers, UV memories, lasers, amplifiers), electrical (e.g. memories, thermistors), and mechanical applications (e.g. gas sensors)¹⁻⁴. Therefore, to improve the industrial processes and help numerical simulation efforts, it is important to know their thermophysical properties. However, the high melting temperatures of these materials pose a risk of contamination and heterogeneous nucleation triggered by impurities coming from the reaction between the corrosive melt and a crucible. This explains why the thermophysical property data of the liquid and supercooled states of oxides are rather scarce^{5,6}. In this study, a hybrid aerodynamic-electrostatic levitation furnace overcame the difficulties associated with high temperature processing and allowed, with the use of an imaging technique, density measurements of these materials in their superheated and supercooled states. The facility and non-contact diagnostic techniques were developed by the Japan Aerospace Exploration Agency as preparatory work for microgravity containerless materials processing in the International Space Station.

¹Japan Aerospace Exploration Agency, Institute of Space and Astronautical Science, 2-1-1 Sengen, Tsukuba, Ibaraki, 305-8505, Japan.

2. Experimental set-up and procedures

The facility used for density measurements (Fig. 1) consisted of a stainless steel chamber housing a hybrid aerodynamic-electrostatic levitator and was operated under a 450 KPa pressure of UHP N₂⁷⁾. An aerodynamic levitator⁸⁾ provided containerless heating of a sample allowing sufficient electrical charges to build-up through thermionic emission to permit subsequent levitation by electrostatic fields (Fig. 2). The electrostatic levitator consisted of a pair of parallel disk electrodes between which the positively charged specimen was kept levitating through an active feedback loop (vertical control)⁹⁾. Four spherical electrodes distributed around the bottom electrode were used for horizontal position control, also through feedback control.

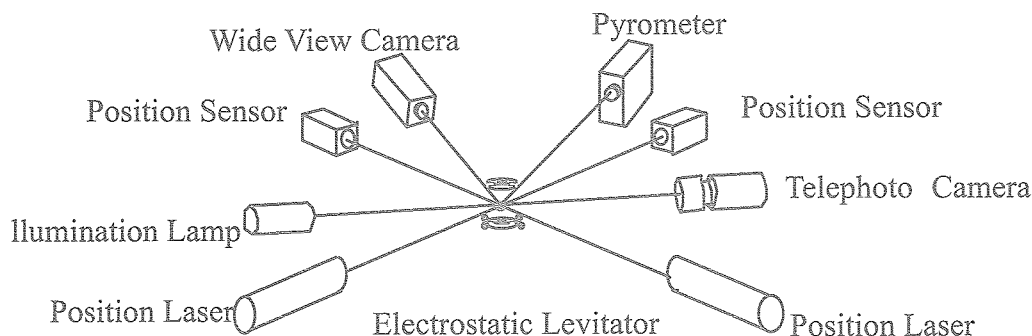


Fig.1. Schematic representation of the facility.

The sample was heated from the above using the unfocused radiation (10.6 mm) coming from a computer controlled 100 W CO₂ laser. Temperature was recorded over wide ranges by pyrometry (0.90 μm, 0.96 μm, 5.14 μm; 120 Hz sampling rate). The apparent temperature, obtained from pyrometry, was calibrated with the release of the latent heat of fusion of the material (recalcescence peak) with the help of Planck's law. Due to the lack of data, the emissivity was set at the melting point for each material and assumed constant at all temperatures.

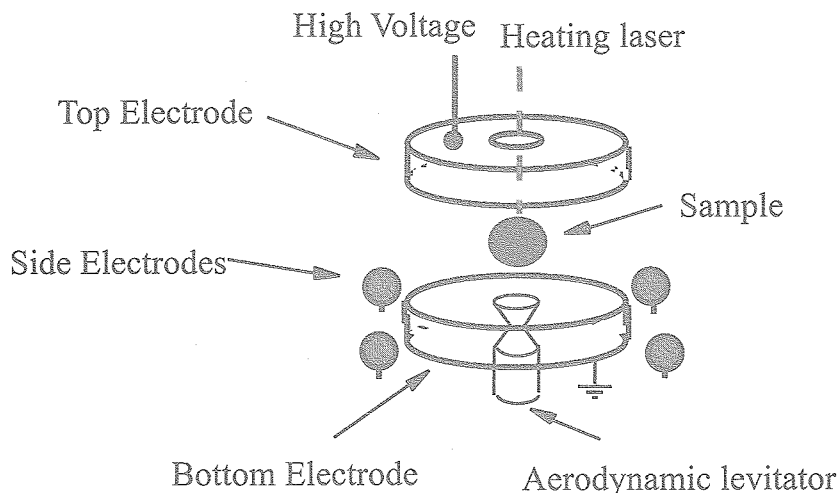


Fig.2. Schematic view of the hybrid electrostatic-aerodynamic levitator

Density measurements were obtained using an imaging technique described in detail elsewhere¹⁰. In short, a high-resolution, black and white charged-coupled-device video camera equipped with a telephoto objective and a high-pass filter at 450 nm was used to obtain a magnified view of the sample illuminated from behind with an intense UV light. The UV spectral range allowed a sharp observation of the rim of the sample even at temperature well above the melting point. Hence, this excellent imaging permitted density measurements for both supercooled and liquid materials. Upon melting, a sample took a spherical shape due to surface tension and the distribution of surface charge. Images at the rate of 30 frames/s (Fig. 3) and temperature data (Fig. 4) were simultaneously recorded and the laser beam was blocked with a mechanical shutter allowing the sample to cool.

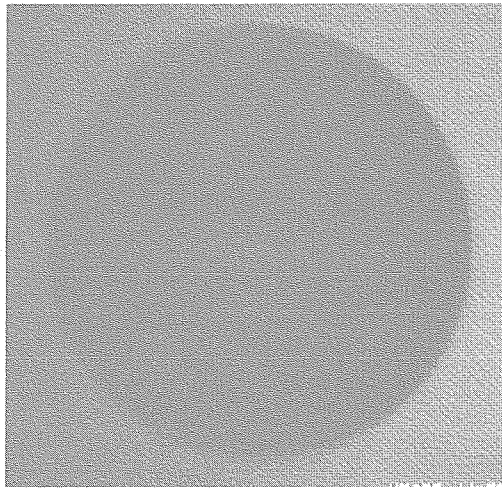


Fig.3. Side view of a levitated and supercooled Nd-CA sample (10.32 mg).

After the experiment, the video images were digitized and the sample radius was extracted from each image. The images were then matched with the corresponding cooling curve, obtained from the temperature data. Since the sample was axi-symmetric, the volume was obtained from the radius, and because its mass was known, the density could be found as a function of temperature. The recorded images were calibrated by levitating a sphere with a precisely known radius under identical experimental conditions. Calculations indicated that the effects of hydrostatic pressure on the sample and variations in the index of refraction due to temperature changes were negligible. In addition to the UV backlighting, the camera was also used with a white light or with no background light to help observe surface features.

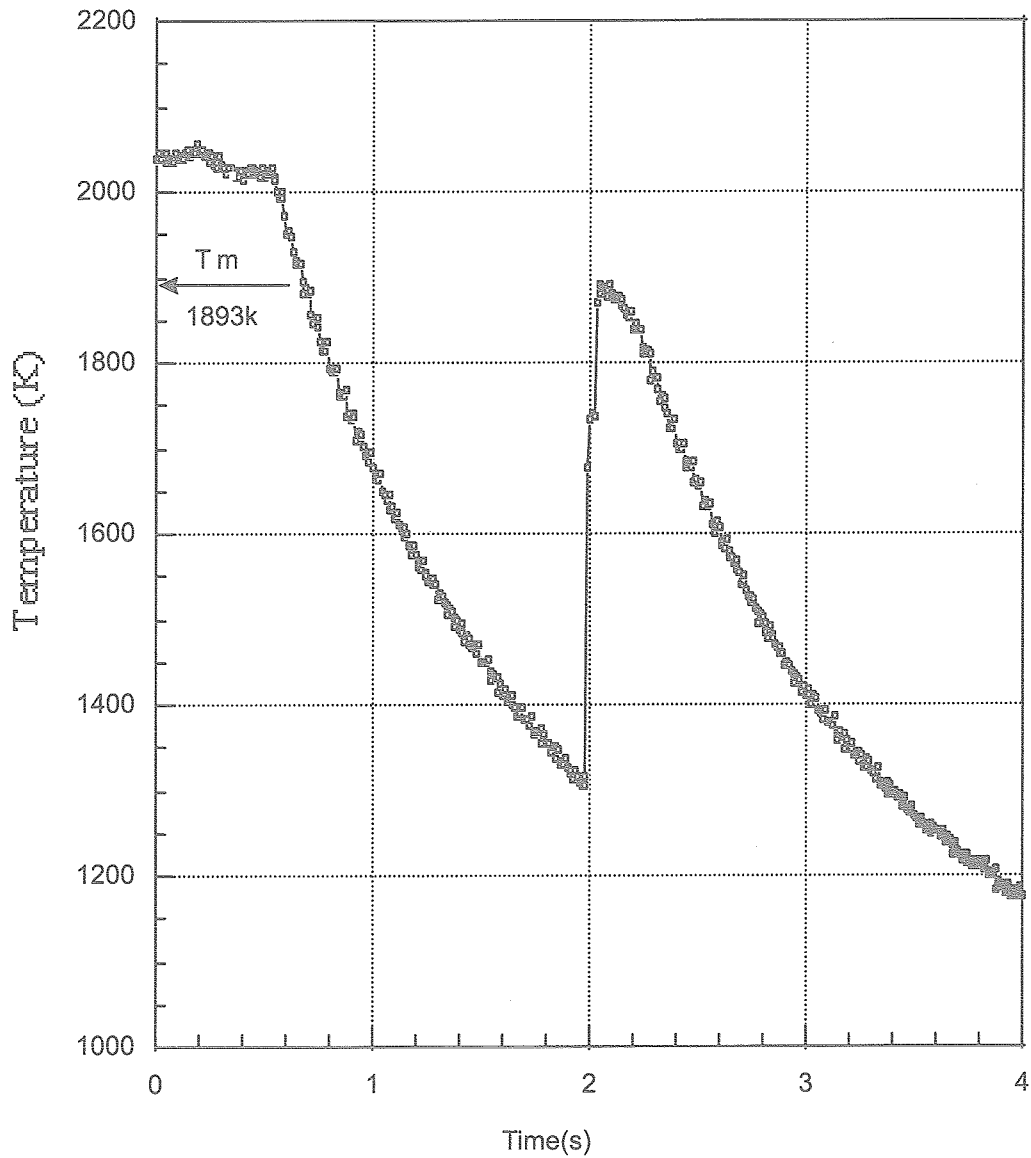


Fig.4. Typical thermogram of a levitated BaTiO₃ sample (12.16 mg).

The work function ϕ of a material can be evaluated using the Richardson-Dushman equation ¹¹⁾,

$$\phi = -kT \ln [J/A T^2] \quad (1)$$

where k is the Boltzmann constant ($1.38 \times 10^{-23} \text{ J.K}^{-1}$), T is the sample temperature, J is the current density, and A is a constant ($120 \text{ A/cm}^2 \text{ K}^{-2}$). Following Weber et al. ¹²⁾, the current density of a sample can be found from by:

$$J = Q/S/t \quad (2)$$

where S is its area, t is the charging time prior to levitation, and Q , the charge of an electrostatically levitated sample, is given by:

$$Q = mg/dE/dz \quad (3)$$

where m is the sample mass, g is the gravitational constant, and dE/dz is the electric field between the two parallel disk electrodes.

3. Results and discussions

3.1. Work function and processing

Samples of several materials (Nd-CA, YAG, BaTiO₃, BiFeO₃) with diameters between 1.6 and 1.82 mm (8.89-16.36 mg) were electrostatically levitated by applying a -7 to -11 kV potential between the disk electrodes. All the data of these experiments were summarized in Table I. From these data and using equation (3), the work function was evaluated at the melting temperature. The data varied from 4.7 for BiFeO₃ to 8.0 for YAG (Table 1). The lack of data for these materials prompted us to assume that the factor A was maximum although it is usually smaller for compounds¹³⁾. Hence, our estimated values for the work function constitute an upper limit. In addition, the uncertainty on the values was estimated to be 20 % considering uncertainties of each measured parameters: electrical field, time prior to levitation, sample surface, mass, and temperature. No data were found in the literature but our values seem plausible when comparing with that for alumina¹³⁾.

Table1. Work function of various ceramics at their melting temperatures.

Material	T _m (K)	Mass (mg)	Diameter (mm)	dE/dz (V/cm)	Work function (eV)
Nd-CA	1878	8.89	1.82	7500	6.7
YAG	2240	12.61	1.80	7000	8.0
BiFeO ₃	1363	16.36	1.60	11000	4.7
BaTiO ₃	1893	12.16	1.70	8000	6.7

Once the sample was levitated, the laser power was gradually increased until the sample was fully melted. The non-rotating sample adopted a spherical shape (Fig. 3) and exhibited excellent position stability. From the magnified images, the amplitude of oscillation was estimated to be less than 50 μm along each direction for all the samples. As the sample cooled, the charge level was a function of the resulting phase. For samples that vitrified, there was a slight charge diminution (less than 10 %) whereas for those that crystallized, the charge loss was substantial and sometimes exceeded the critical value needed to maintain levitation. Upon reheating the solidified samples, small vertical oscillations occurred for a period of 1-2 seconds before stable levitation was restored. As the temperature was further increased, the samples recovered their original stability. For all samples, it was possible to perform numerous superheating-supercooling-solidification cycles while maintaining an adequate sample positioning stability. Fig. 4 shows a typical thermogram for a BaTiO₃ sample, displaying an average combined radiative and convective cooling rate of nearly 470 K/s. The recalescence peak indicated sample crystallization and the high signal to noise ratio illustrated the excellent sample position stability.

Bubbles were sometimes observed when the samples were first melted. These bubbles were quite mobile in the low viscosity liquids and burst at the surface of the levitated drop soon after melting. The recovered samples of all ceramics were approximately spherical and did not show any evidence of voids or bubbles. Recovered Nd-CA and YAG samples were smooth and vitreous. All the samples showed negligible mass loss after the processing experiments that lasted less than 20 minutes.

3.2. Density measurements¹⁴⁻¹⁶⁾

The densities of Nd-CA, YAG, BiFeO₃, and BaTiO₃ were measured over very wide temperature intervals. The data (density at the melting temperature and temperature coefficient) are summarized in Table 2¹⁴⁻¹⁶⁾.

In these measurements, the uncertainty was estimated to be 5 % in the calculation of sample volume based on

Table II. Density of various ceramics in their liquid and supercooled states.

Material	T_m (K)	$\rho(T_m)$ (kg m^{-3})	$d\rho/dT$ ($\text{kg m}^{-3}\text{K}^{-1}$)	Temp. range (K)
Nd-CA	1878	2830	-0.21	1560 - 2000
YAG	2240	4080	-0.29	1470 - 2420
BiFeO ₃	1363	6740	-1.31	1250 - 1490
BaTiO ₃	1893	4040	-0.34	1300 - 2025

the optical resolution of the video imaging system and 1.6 % from the uncertainty in sample mass. In all cases, the variation of density with temperature was linear. Furthermore, for Nd-CA and YAG, the variation of density with temperature was a continuous function with no evidence of a discontinuity at the melting temperature of the crystal, characteristic of glass formation. The Nd-CA data¹⁴⁾ covered the superheated region by more than 120 K, extended 320 K into the supercooled region. At the melting temperature (T_m) of the crystalline phase, our density datum was 2.1 % smaller than that measured by Courtial et al. using the double-bob Archimedean technique¹⁷⁾ and our temperature coefficient agreed with theirs when the experimental uncertainties of both studies were taken into account.

For YAG¹⁵⁾, the data included approximately 180 K of superheat and extended 770 K into the supercooled region. The density at T_m was 8.1 % larger than that of ref. 18 measured with the double-bob technique and our temperature coefficient was 4.5 times larger than the value reported in ref. 18.

For BiFeO₃¹⁶⁾, the data covered 127 K above T_m and extended 183 K into the supercooled region. Besides the datum reported by Murashov et al.¹⁹⁾ at T_m , which agreed within 20% with our value, no other data were available in the literature.

Similarly, for BaTiO₃¹⁶⁾, the data extended more than 132 K above the melting point and 593 K into the supercooled region. To the best of our knowledge, these measurements were the first to be reported on such a large temperature interval, in particular in the supercooled state.

The discrepancy observed between our results and those of refs. 17-19 could be attributed to the measuring techniques. We used non-contact and imaging methods in a pressurized air atmosphere that isolated our sample from container walls and hence prevented any contamination. Therefore, possible sources of error could arise from the focusing of the sample image, the digitization of the image, and the measurements of sample mass. In addition, since the viscosity of the liquid increases significantly as temperature decreases, it is expected that the density data measured at lower temperatures will have a larger uncertainty because any deformation of the sample will not be recovered on the time scale of the measurements. Some investigators used the Archimedean method for which possible convection in samples could have caused the apparent bob weight to vary^{17,18)}. Thermal gradients in their samples could also have occurred. No details on the measurement technique and on uncertainties being given in ref. 19, it is difficult to explain the discrepancy observed for BaTiO₃.

4. Conclusions

The work function of several molten ceramics (Nd-CA, YAG, BaTiO₃, BiFeO₃) was evaluated using the Richardson-Dushman equation. In addition, the densities of these materials in their liquid and supercooled phases were reported over very wide temperature intervals. The data presented in this research were obtained from temperature profiles and image acquisition. Therefore, to improve the data, efforts are focused towards ways to

increase image sharpness and contrast, and to obtain better temperature readings. Reduction in the scatter of the data might help resolve the expected changes in the liquid density due to the structural changes occurring at the glass transition. Measurements of the density of CaF_2 and $76\%\text{BaB}_2\text{O}_4\text{-}24\%\text{Na}_2\text{O}$ are currently underway and will be reported elsewhere. Parallel activities are also devoted on ways to implement isobaric heat capacity, surface tension, and viscosity measurement techniques.

Although several successes were achieved over the years on the ground with the pressurized electrostatic levitation furnace, difficulties are faced when handling some oxides due to insufficient charges before reaching the melting point or sudden charge loss at melting, leading to an interruption in levitation. Microgravity would ease non-contact positioning of such materials while providing a quiet hydrodynamic environment. Also, limitation on the magnitude of electric field between the electrodes and the risk of electrical breakdown while using the oscillation drop technique complicates viscosity and surface tension determination on the ground. Microgravity would alleviate this problem and facilitate these property measurements. Microgravity experiments would, in addition, offer an attractive platform for solidification studies.

Acknowledgments

The authors are grateful to Dr. A. Douy (CNRS France) for synthesis of Nd-CA materials and to Dr. J.-M. Gagné (École Polytechnique, Montréal) and to Dr. J.K.R. Weber (Containerless Research Inc.) for providing some of the materials. Sincere thanks also to Dr. J. Yu (JAXA) for help in some experiments.

References

- [1] J.E. Shelby, *J. Amer. Ceram. Soc.*, **68**, 155 (1985).
- [2] A.A. Kaminskii, *Crystalline Lasers*, CRC Press, Boca Raton, 1996.
- [3] B.U.M. Rao and G. Srinivasan, *Phys. Rev. B*, **44** (1991), 395.
- [4] N. Huot, J.M.C. Jonathan, G. Pauliat, D. Rytz, and G. Roosen, *Opt. Comm.* **135** (1997), 133.
- [5] B. Granier and S. Heurtault, *Rev. Int. Hautes Temp. Refract.*, **20** (1983), 31.
- [6] B. Glorieux, F. Millot, J.-C. Rifflet, and J.-P. Coutures, *Int. J. Thermophys.*, **20** (1999), 1085.
- [7] P.-F. Paradis, T. Ishikawa, J. Yu, and S. Yoda, *Rev. Sci. Instrum.* **72** (2001), 2811.
- [8] P.-F. Paradis, F. Babin, J.-M. Gagné, *Rev. Sci. Instrum.*, **67** (1996), 262.
- [9] W.-K. Rhim, S.-K. Chung, D. Barber, K.F. Man, G. Gutt, A.A. Rulison, and R.E. Spjut, *Rev. Sci. Instrum.* **64** (1993), 2961.
- [10] T. Ishikawa, P.-F. Paradis, and S. Yoda, *Rev. Sci. Instrum.* **72** (2001), 2490.
- [11] C. Kittel, *Introduction to Solid State Physics*, 6th edition, John Wiley and Sons, New-York, 1986, p.536.
- [12] J.K.R. Weber, J. Tangeman, T. Key, K. Hiera, P.-F. Paradis, T. Ishikawa, J. Yu, S. Yoda, *Jpn. J. Appl. Phys.*, **41**, Pt.1, (5A) (2002), 3029-3030.
- [13] E.A. Brandes and G.B. Brook, *Smithells Metals Reference Book*, 7th ed., Butterworth-Heinemann Ltd., Oxford, 1992.
- [14] P.-F. Paradis, J. Yu, T. Ishikawa, S. Yoda, *J. Am. Ceram. Soc.* **86** (2003), 2234-2236 .
- [15] P.-F. Paradis, J. Yu, T. Ishikawa, T. Aoyama, S. Yoda, J.K.R. Weber, *J. Cryst. Growth*, **249** (2003), 523.
- [16] P.-F. Paradis, J. Yu, T. Ishikawa, T. Aoyama, S. Yoda, *Appl. Phys. A*, **79** (2004), 1965-1969.
- [17] P. Courtial and D.B. Dingwell, *Geochim. Cosmochim. Acta*, **59** (1995), 3685-3695.
- [18] V.J. Fratello and C.D. Brandle, *J. Cryst. Growth*, **128** (1993), 1006.
- [19] V.A. Murashov, D.N. Rakov, V.M. Ionov, I.S. Dubenko, Y.V. Titov, and V.S. Gorelik, *Ferroelectric*, **162** (1994), 11.

**JAXA Research and Development Report
(JAXA-RR-04-023E)**

Date of Issue : Mar 31, 2005

Edited and Published by :
Japan Aerospace Exploration Agency
7-44-1 Jindaiji-higashimachi, Chofu-shi,
Tokyo 182-8522 Japan

Printed by :
FUJIWARA PRINTING Co., Ltd.
3-6-4 Fujimidai, Kunitachi-shi, Tokyo 186-0003 Japan

© 2005 JAXA, All Right Reserved

Inquires about copyright and reproduction should be addressed to the
Aerospace Information Archive Center, Information Systems Department
JAXA. 2-1-1 Sengen, Tsukuda-shi, Ibaragi 305-8505 Japan.

